



HAL
open science

A Performance Analysis of Optimization Algorithms for Wiring Network Reconstruction and Diagnosis based on Reflectometry

Moussa Kafal, Wafa Ben Hassen, Jaume Benoit

► **To cite this version:**

Moussa Kafal, Wafa Ben Hassen, Jaume Benoit. A Performance Analysis of Optimization Algorithms for Wiring Network Reconstruction and Diagnosis based on Reflectometry. 2019 International Automatic Testing Conference (AUTOTESTCON), Aug 2019, National Harbor, United States. pp.8961070, 10.1109/AUTOTESTCON43700.2019.8961070 . cea-03049343

HAL Id: cea-03049343

<https://cea.hal.science/cea-03049343v1>

Submitted on 14 Dec 2020

HAL is a multi-disciplinary open access archive for the deposit and dissemination of scientific research documents, whether they are published or not. The documents may come from teaching and research institutions in France or abroad, or from public or private research centers.

L'archive ouverte pluridisciplinaire **HAL**, est destinée au dépôt et à la diffusion de documents scientifiques de niveau recherche, publiés ou non, émanant des établissements d'enseignement et de recherche français ou étrangers, des laboratoires publics ou privés.

A Performance Analysis of Optimization Algorithms for Wiring Network Reconstruction and Diagnosis based on Reflectometry

Moussa KAFAL^{*}, *Member, IEEE*, Wafa BEN HASSEN^{*}, and Jaume BENOIT^{*}

^{*}CEA, LIST, Laboratoire de Fiabilité et Intégration Capteurs, 91191 Gif-sur-Yvette, France.
moussa.kafal@cea.fr

Abstract—During the last decade, time domain reflectometry (TDR) methods have formed the cornerstone for the diagnosis of transmission line networks. They have been adopted recently to the blind characterization of networks, thanks to graph theory and optimization based algorithms. Using a single testing point, it became possible to reconstruct the topology of a black-boxed network while returning precise estimates of branch lengths and most importantly load impedances. In other words, disconnecting the network for testing purposes is no longer needed. In this paper, we opted to perform a comparative analysis to study the effect of different optimisation based algorithms on the applicability of the aforementioned method. Particularly, we designed CAN bus networks based on real aeronautical cables of increased complexity to investigate their performance in terms of precision and computational burden.

Index Terms—Complex wire networks; topology reconstruction; inverse problems; optimisation algorithms.

I. INTRODUCTION

In the era of Internet of Things (IoT), electrical wiring and interconnect systems (EWIS) are massively hosted everywhere in many fields such as transportation systems, communication networks, power grids, etc., where the transfer of energy and information is a fundamental pillar to ensure the optimal system operation [1]. Yet wiring faults and failures originated from aging, corrosion and vandalism, etc., are inevitable and can lead to problems with the quality of power and communication, blackouts, aircraft crashes, and fires, etc.

Much research has been done to determine viable methods for the location of wiring faults. This effort has been spurred on by catastrophic accidents that has occurred. A reliable method for locating wiring problems is needed for the safety of the general public. With life and limb at stake, the expense of maintaining faulty wiring is a driving force in funding the development of better fault location methods. Currently, several methods are available to determine wire fault locations.

The most widely used technique is reflectometry. Thereby, a high-frequency signal is injected into the network under test (NUT) [2]. The reflected signal is rich of information about changes of cable impedances which is in turn valuable to monitor wiring faults. Over the last decade, many variants of reflectometry have been developed targeting specific applications and trying to bypass inherent limitations. This included the well known Time Domain Reflectometry (TDR) [3], Frequency Domain Reflectometry (FDR) [4], Ultra Wide Band (UWB) based TDR [5], and Spectrum Time Domain Reflectometry (STDR) [6], etc. They use different incident signal and signal processing methods.

Raw reflectometry data can be quite complicated and very difficult to analyze once branched networks are addressed [7]. In fact, this is mainly caused by junctions, network terminations, etc. that lead to the occurrence of multiple reflections. On the other hand, improved reflectometry methods used the baseline approach to bypass this problem. In baselining, the reflectometry response of the faulty NUT is compared with that of a reference healthy version of it, which can be either retrieved by measurements or computed from simulations. This operation ideally removes the spurious echoes generated by impedance discontinuities like junctions, leaving only those echoes initially generated by the interaction between the testing signals and the faults in order to enable the detection, location, and characterization of different types of faults [8].

Accordingly, mapping the tested network is a direct way to diagnose faults. In fact, this would allow reconstructing the topology of a totally or partially unknown network, and thus serve as a reference healthy model of the NUT. This will later form the basis of baselining for reflectometry methods enabling continuous monitoring of an EWIS. Besides, most fault detection techniques outside the scope of reflectometry also rely on the prior knowledge of the network's topology for their proper applicability [9].

Within this context, considerable work has been realized in the state-of-art towards developing and optimizing techniques dedicated for wired network mapping [10], [11]. A vast majority relied on the tenets of reflectometry to measure the response of a tested network from one or more of its extremities [12]. This was followed by solving the inverse problem, where a response provided by a direct model is iteratively improved to finally align with the measured response. This became possible, thanks to the wide selection of optimization algorithms.

In literature, many authors have been working on merging reflectometry with different optimization based techniques for the sake of EWIS mapping [13]–[15]. However, most relied on the prior knowledge of the network's topology and were confined to estimating the branch lengths. Besides, predefined loads were imposed at the extremities of the tested network which were mainly open or short circuits. In practice, disconnecting the network from its loads is unattainable in many applications (nuclear power-plants, aeronautics, etc.), and the beforehand awareness of its scheme is generally impossible.

In a recent development, the authors of [16]–[18], proposed integrating the graph theory with the optimization based algorithms to solve the inverse problem of measured TDR

responses for totally unknown networks. These joint graph-optimization-reflectometry (GOR) techniques enabled a blind reconstruction of the tested network accompanied with estimating branch lengths and returning precise assessment of the load impedances.

The present paper, is intended to present a full-scale comparative study of several optimization techniques in the GOR method and investigate thoroughly the advantages and disadvantages of each as a function of several parameters including the computational time, complexity of the network, hardware implementation, accuracy, etc. The study will be backed up with experimental validations using real-life complex wiring networks.

II. METRICS OF THE GOR BASED METHODS

The GOR methods have shown to be efficient in mapping obscure wiring networks using a single-extremity measured TDR response followed by resolving the inverse problem. In what follows we will try to explain different elements and stages composing these techniques.

A. Wave Propagation Model

A direct model is capable of describing the propagation of high frequency electromagnetic waves along a Transmission Line TL in the time domain: the model is based on the telegrapher's equations given by (1a) &(1b), where the per-unit-length electrical parameters matrices R , L , C and G are computed by a Finite Element Method FEM [19].

$$\frac{\partial v(x, t)}{\partial x} = -Ri(x, t) - L \frac{\partial i(x, t)}{\partial t} \quad (1a)$$

$$\frac{\partial i(x, t)}{\partial x} = -Gv(x, t) - C \frac{\partial v(x, t)}{\partial t} \quad (1b)$$

Despite the fact that time domain analysis as the Finite Difference Time Domain method (ABCD) provides accurate full-wave solutions over large frequency bands, they can be computationally heavy, slow and inefficient. On the contrary, frequency domain techniques, particularly, the ABCD matrix method offers excellent fidelity and computational efficiency since they avoid the explicit use of differential equations [20]. An important advantage of this approach is that the transmission line modelling arises naturally in the frequency domain. Therefore the consideration of frequency dependent parameters can be carried out in a simple way compared with the time-domain.

ABCD parameters, also known as the transmission line parameters, provide the link between the supply and receiving end voltages and currents of a two-port network model. In fact, any transmission line branch can be modeled as such. The two-port network is regarded as a "black box" with its properties specified by a matrix of numbers. This allows the response of the network to signals applied to the ports to be calculated easily, without solving for all the internal voltages and currents in the network.

Since we are dealing with NUTs of tree-like structures, ABCD matrix method makes it possible to analyze such

networks, thanks to its cascading property. As such, each branch composing a NUT could be separately analyzed and then cascaded with other branches splitting from it to return the overall behavior of the NUT. With this in mind, an in-house solver developed at CEA under MATLAB provided an accurate model of reflectometry responses for any branched network. Accordingly, the simulated TDR response of the NUT model is simply the inverse Fourier transform (IFFT) of the computed end voltage.

Having derived a direct model to provide the simulated TDR response of an assigned NUT, solving the inverse problem of the measured TDR response of the unknown network entails several variable sets. This includes the NUT's topology, the branch lengths and the load impedances.

B. Branched network as a Graph

Network topology is a generic name that refers to all properties arising from the structure or geometry of a network. If each element or a branch of a network is represented on a diagram by a line irrespective of the characteristics of the elements, we get a graph. Hence network topology is network geometry. Thus topology deals with the way in which the various elements are interconnected at their terminals without considering the properties and type of the elements connected. This method is considered to be a more systematic approach to the analysis of branched TL networks.

The Graph theory forms a convenient mathematical representation of a network describing the relationship between lines and points [21]. As such, a graph is a pair of sets $\mathbf{G} = (\mathbf{N} \mathbf{Ed})$, where \mathbf{N} is a set of vertices or nodes and \mathbf{Ed} is a set of edges formed by pairs of nodes [22]. Accordingly, a tree-like TL network can be represented by a graph whose nodes \mathbf{N} are loads and junctions while the edges \mathbf{Ed} are the TL branches connecting the nodes. A hypothesized numerical model of a generic network can thus be set based on the tenets of Graph theory, whose components are to be iteratively changed to meet those of the measured network. This an inverse problem to be solved.

C. Solving the Inverse Problem

The term "inverse problem" is generally understood as the problem of finding a specific physical property, or properties, of the medium under investigation, using indirect measurements [23]. It can be seen as the reverse process of a forward problem, which concerns with predicting the outcome of some measurements given a complete description of a physical system. In our case study, having measured the TDR response of an unknown TL network, retrieving the network's parameters (topology, branch lengths, and load impedances) is possible by solving this inverse problem.

Optimization algorithms are central approaches in solving inverse problems as the recovery of the unknown parameters is formulated as an optimization problem [24]. An optimization problem consists in maximizing or minimizing some function relative to some set, representing a range of choices available

in a certain situation. The function allows comparison of the different choices for determining which might be best.

More formally we define the optimization problem as

$$\text{optimize } f(x), x \in S \quad (2)$$

where *optimize* stands for *min* or *max* $f : \mathbb{R}^n \rightarrow \mathbb{R}$ denotes the objective function, that we assume throughout at least continuously differentiable, and $S \subseteq \mathbb{R}^n$ is the feasible set, namely the set of all admissible choices for x . x represents in our investigation the set of the NUT graph's variables, namely N and Ed . To obtain the best candidate solutions that mostly align with the actual tested network, we will solve the optimization problem of the following objective function

$$F_{\text{obj}} = \int_{t=0}^{\infty} \frac{\|\mathbf{V}_s(t) - \mathbf{V}_m(t)\|_2}{1+t^2} dt \quad (3)$$

with $\mathbf{V}_s(t)$ and $\mathbf{V}_m(t)$ being the time domain reflectometry responses of the hypothesized simulated and measured networks, respectively. From now on-wards, the temporal variable t will be dropped for the sake of simplicity. Fig. 1 presents a mesh plot of the objective function evaluation of eq. 3 for a single point-to-point network with N being a single load impedance, while E_d being the length of the sole branch. Notably, the function appears to be non-convex with several minima and maxima. Indeed, the situation is expected to worsen with complex branched networks composed of several junctions connecting numerous branches and terminated with a number of loads.

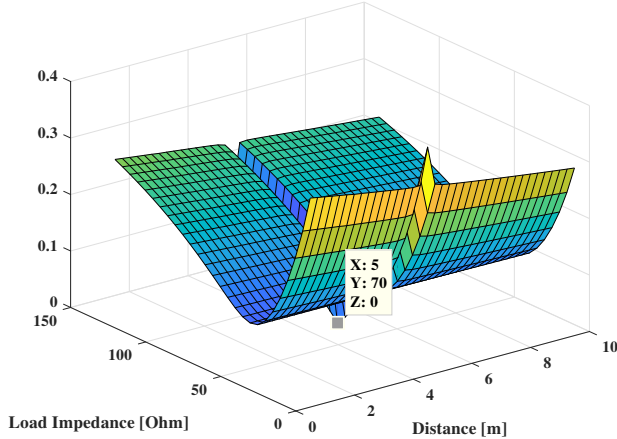


Fig. 1: A mesh plot of the fitness function evaluation of a single branch network.

To cope with such a problem, global optimization algorithms are efficient numerical techniques capable of solving inverse problems with non-convex objective functions suffering from local minima and maxima [25]. In fact, they have shown promising results in converging to the function's global minimum or maximum.

Accordingly, we have adopted several global optimization algorithms in our study namely, the genetic algorithm (GA) as

in [17], [26], [27], particle swarm algorithm (PSO) as done in [16], in addition to the surrogate (SG) and simulated annealing (SA) algorithms for the first time to such application. The purpose is to conduct a performance analysis to compare the results obtained when applying each of the considered optimization algorithms relative to several parameters as NUT's complexity, computational time, etc. In what follows we will briefly explain each of the considered algorithms.

1) *Genetic algorithm*: GAs are adaptive heuristic search algorithms based on the evolutionary ideas of natural selection and genetics [28]. As such, they represent an intelligent exploitation of a random search used to solve optimization problems. GAs simulate the survival of the fittest by starting with a random sample set (initial population) of potential solutions (chromosomes). Each chromosome is coded as a finite length vector of variables which are analogous to genes. These solutions then undergo recombination and mutation (like in natural genetics), producing new children, and the process is repeated over various generations. Each individual (or candidate solution) is assigned a fitness value (based on its objective function value) and the fitter individuals are given a higher chance to mate and yield more "fitter" individuals until an eventual convergence is reached. As a result, an optimal population is produced that will now contain the optimal solutions.

2) *Particle swarm algorithm*: PSO is a relatively recent heuristic search approach founded on the concept of swarm intelligence (SI) that is based on the idea of collaborative behavior and swarming in biological populations [29]. As a population-based technique, PSO is regarded to be conceptually simple as only few parameters need to be regulated. The population, often referred to as swarm, is composed of n candidate solutions known as particles. Each particle $i = 1, 2, 3, \dots, n$ in the swarm space has an identity defined by its position p_i , in addition to its moving velocity v_i . In fact, the displacement of a particle in space is controlled by a well defined strategy based on its own best known position $pbest_i$ as well as the global best known position $gbest_i$ of the entire swarm. Equations 4 summarize the moving mechanism. It is important to note that, w_i is the inertia weight specific to each particle, r_1 & r_2 are random numbers uniformly generated between $[0, 1]$, while c_1 & c_2 are learning acceleration factors.

$$\begin{aligned} v_i^{t+1} &= w_i v_i^t + c_1 r_1^t (pbest_i^t - p_i^t) + c_2 r_2^t (gbest_i^t - p_i^t) \\ p_i^{t+1} &= p_i^t + v_i^{t+1} \end{aligned} \quad (4)$$

As an illustration, the particles' convergence towards the best solution is likely determined by their fitness which is controlled by a predefined objective function F_{obj} specific to each application. Namely, the position p_i determines each particle's fitness that is updated regularly at each iteration *iter* of the PSO algorithm according to what has been defined in equations 4. The process is repeated until a specific criterion is reached which might be the maximum number of iterations, the stalking state time after which no improvements can be detected, etc.

3) *Surrogate optimization algorithm*: SG is a global solver for time-consuming objective functions [30]. It is black-box optimization technique that is well-suited for problems whose objective functions are very expensive to evaluate with no analytical or derivative information available. The main idea of SG is to iteratively construct models to approximate the black-box functions (globally) and use them to search for optimal solutions. A common simple-form approach for surrogate-based methods is as follows:

- Phase 1 (design): Let $k := 0$. Select and evaluate a set S_0 of starting points.
- While some given stopping criteria are not met:
 - . Phase 2 (model): From the data $(x, f(x)) | x \subseteq S_k$, construct a surrogate model $s_k(\cdot)$ that approximates the black-box function.
 - . Phase 3 (search): Use $s_k(\cdot)$ to search for a new point to evaluate. Evaluate the new chosen point, and update the data set S_k . Assign $k := k + 1$.

4) *Simulated annealing algorithm*: SA is an optimization method which mimics the slow cooling of metals, that is characterized by a progressive reduction in the atomic movements that reduce the density of lattice defects until a lowest-energy state is reached [31]. In a similar way, at each virtual annealing temperature, the simulated annealing algorithm generates a new potential solution (or neighbour of the current state) to the problem considered by altering the current state, according to a predefined criterion. The acceptance of the new state is then based on the satisfaction of the Metropolis criterion, and this procedure is iterated until convergence.

It has been proved that by carefully controlling the rate of cooling of the temperature, SA can find the global optimum. SA's major advantage over other methods is an ability to avoid becoming trapped in local minima. The algorithm employs a random search which not only accepts changes that decrease the objective function, but also some changes that increase it.

D. GOR method implementation

The flowchart shown in Fig. 2, illustrates the step-by-step the GOR procedure proposed to blindly reconstruct unknown networks. As can be seen, it starts by measuring the TDR response \mathbf{V}_m of the tested NUT using one extremity while others are left connected to their loads. Indeed, measuring the reflectometry response can be accomplished by connecting the testing extremity of the NUT to one of the ports of a vector network analyzer (VNA), the TDR response is simply the IFFT of the scattering parameter S_{11} . However, that is also possible by relying on any of the existing reflectometry measuring devices.

Once \mathbf{V}_m is collected, solving the inverse problem commences by adopting graph theory to generate a generic network model with two sets of variables \mathbf{N} and \mathbf{E}_d . The in-house TL line solver described in sec. II-A is devoted to return the TDR response \mathbf{V}_s of any hypothesized NUT. \mathbf{N} and \mathbf{E}_d are then iteratively changed, thanks to global optimization techniques, until convergence occurs between \mathbf{V}_s and \mathbf{V}_m ,

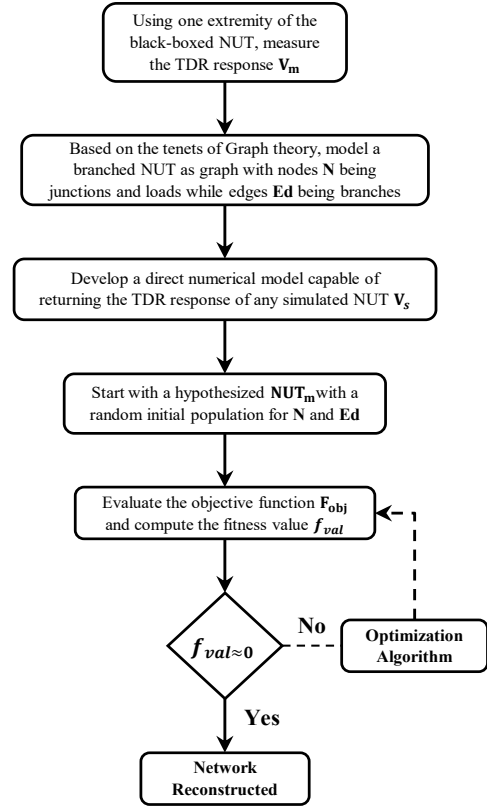


Fig. 2: Flowchart of GOR methods.

i.e. the minimal fitness value of \mathbf{F}_{obj} is reached. This marks the proper reconstruction of the tested unknown network, by retrieving its topology, branch lengths and load impedances.

III. PERFORMANCE ANALYSIS

A experimental setup based on practical industrial elements is conducted in order to serve as a profound demonstration for comparing the performance of the proposed GOR approach relative to different optimization algorithms. Three different complexity NUTs will be tested. Although, they can't cover the entire range of possible combination of networks, but they are mostly found in practice.

A. Experimental setup

Figs. 3 show the three NUTs considered in our study. They are Controller Area Network (CAN) bus NUTs commonly used in aeronautics due to their reliability for data communication in mission and safety critical applications in aircrafts. The least complex structure is a single Y-junction network and the most complex is an NUT composed of 7 branches connected via two junctions. The networks are designed using $RG-316$ 50Ω coaxial cables. For simplicity, passive element resistors with randomly chosen impedances were created to serve as loads. In fact, this does not bring any limitation to the application of our method, as any other kind of passive loads could be considered. The testing port of each network

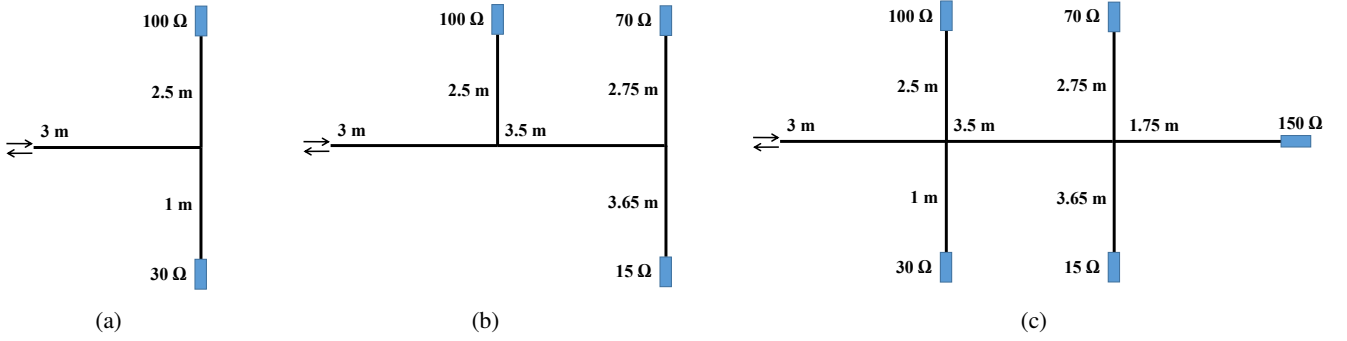


Fig. 3: Topologies of the CAN bus wire networks used for the experimental validation of the GOR method with (a): single Y-junction, (b) double Y-junction 5 branch, and (c) double Y-junction 7 branch networks.

was connected to an E5071C KEYSIGHT VNA covering a frequency range from 9.5 KHz to 4.5 GHz. Acquisition was done over a total bandwidth of 2 GHz, a frequency step 1 MHz, an intermediate-frequency filter bandwidth set to 100 kHz and an input power set to a 0-dBm harmonic excitation signal. The time domain TDR response \mathbf{V}_m is obtained by applying an IFFT to the measured frequency domain S_{11} parameter.

B. Result discussion

Having acquired \mathbf{V}_m for each NUT of Figs. 3, the GOR algorithm detailed in sec. s applied. Each of the aforementioned optimization algorithms explained in sec. II-C is enforced at a time. Executing the GOR procedure was accomplished using a state-of-art PC employing an Intel 2.53 GHz CPU processor.

Regardless the optimization algorithm deployed, the proposed GOR methodology was capable of correctly returning the network's topology. However, the processing time differed from one to another, as well as the estimated branch lengths and load impedances. In order quantify the obtained results, we opted to compute $\Delta_L = (|(L_a - L_r)/L_a|) \times 100$ and $\Delta_Z = (|(Z_a - Z_r)/Z_a|) \times 100$, the length and impedance % errors respectively. L_a and Z_a are the actual NUT branch lengths and load impedances, while L_r and Z_r are the reconstructed ones. T is the time needed to execute the GOR process. Fig. 4 presents a reflectogram showing the measured \mathbf{V}_m and reconstructed \mathbf{V}_s TDR responses after applying the GOR procedure implementing the GA algorithm on the single Y-junction NUT of Fig. 3 (a). Actually, the right topology was identified and precise estimates of the branch lengths and load impedances were obtained which can be noticed from the close agreement between \mathbf{V}_m and \mathbf{V}_s .

Tables I, II, III& IV display a qualitative assessment of Δ_L , Δ_Z , and T for each of the three NUTs of Figs. 3 with respect to the optimization algorithm deployed. Several features need to be commented. First of all, as already stated the right NUT topology was eventually reconstructed. Besides, it can be noticed that the length error Δ_L doesn't exceed 2.8% for the single Y-junction NUT for all adopted optimization algorithms. GA and PSO appear to outperform SG and SA algorithms with a Δ_L below 0.5%, i.e. a roughly 8 mm change estimate from the actual branch length. Although, it is

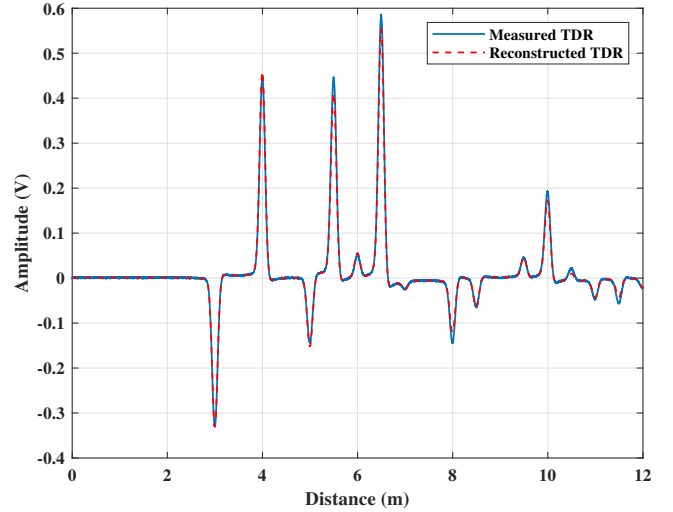


Fig. 4: The measured and simulation-reconstructed TDR reflectometry responses of the unknown network of Fig. 3(a).

expected that this error increases with an increased complexity of the network addressed, PSO does not over-top the 1% length error even with the double Y-junction 7 branch NUT, which is a remarkably great result. However, SG and SA show a deteriorated performance with Δ_L escalating to 7.5% for the NUT of Fig. 3(c).

Estimating the impedances of loads at the extremities seems to be a harder task, where results obtained show a Δ_Z reaching over 70% for the double Y-junction 7 branch network with the SA algorithm. Nevertheless, the PSO algorithm keeps an impedance error not exceeding 15%, which is quite acceptable for the reconstruction of loads.

Noteworthy, the adopted algorithms show efficiency in terms of the total duration needed for post-processing with a maximum latency below half an hour for the most complex network studied. Particularly, PSO needs no more than 3.5 minutes when testing the 7 branched network. Particularly, the vast majority of NUTs in aeronautical applications have structures that do not surpass in complexity the three considered topologies.

Single Y-Junction NUT												
Algo.	L_1 (3 m)		L_2 (2.5 m)		L_3 (1 m)		Z_1 (100 Ω)		Z_2 (30 Ω)		T	
GA	3.005	0.16%	2.492	0.32%	1.008	0.8%	108	8%	27	10%	48 s	
PSO	2.999	0.03%	2.498	0.08%	0.997	0.03%	102	2%	31	3.3%	30 s	
SG	2.991	0.3%	2.485	0.6%	1.010	1%	112	12%	22	26%	65 s	
SA	2.989	0.36%	2.512	0.48%	0.972	2.8%	117	17%	39	30%	90 s	

TABLE I: Table showing the actual and estimated branch lengths and load impedances for the NUT of Fig. 3 (a) with the computing time.

Double Y-Junction 5-Branch NUT																	
Algo.	L_1 (3 m)		L_2 (2.5 m)		L_3 (3.5 m)		L_4 (2.75 m)		L_5 (1 m)		Z_1 (100 Ω)		Z_2 (70 Ω)		Z_3 (15 Ω)		T
GA	3.006	0.2%	2.491	0.36%	3.485	0.42%	2.759	0.32%	0.992	0.8%	110	10%	82	17%	18	20%	2.5 min
PSO	2.998	0.06%	2.505	0.2%	3.488	0.34%	2.748	0.07%	1.002	0.2%	105	5%	76	8.5%	16	6.6%	1.5 min
SG	2.992	0.26%	2.483	0.68%	3.530	0.85%	2.760	0.36%	1.019	1.9%	122	22%	84	20%	10	33.3%	4 min
SA	3.098	3.2%	2.515	0.6%	3.600	2.85%	2.685	2.36%	0.958	4.2%	75	25%	40	30%	24	60%	7.5 min

TABLE II: Table showing the actual and estimated branch lengths and load impedances for the NUT of Fig. 3 (b) with the computing time.

Double Y-Junction 7-Branch NUT														
Algo.	L_1 (3 m)		L_2 (2.5 m)		L_3 (1 m)		L_4 (3.5 m)		L_5 (2.75 m)		L_6 (3.65 m)		L_7 (1.75 m)	
GA	3.009	0.3%	2.488	0.48%	0.987	1.3%	3.455	1.28%	2.725	0.9%	3.69	1.1%	1.79	2.28%
PSO	3.005	0.16%	2.511	0.44%	1.009	0.9%	3.532	0.91%	2.765	0.54%	3.635	0.4%	1.662	0.72%
SG	3.090	3%	2.475	1%	1.040	4%	3.430	2%	2.653	3.5%	3.496	4.2%	1.687	3.6%
SA	2.88	4%	2.437	2.5%	0.94	6%	3.307	5.5%	2.598	6.5%	3.387	7.2%	1.618	7.5%

TABLE III: Table showing the actual and reconstructed branch lengths for the network of Fig. 3 (c).

Double Y-Junction 7-Branch NUT											
Algo.	Z_1 (100 Ω)		Z_2 (30 Ω)		Z_3 (70 Ω)		Z_4 (15 Ω)		Z_5 (150 Ω)		T
GA	115	15%	24	20%	58.8	16%	19	26.6%	180	20%	6 min
PSO	109	9%	33	10%	69	12.8%	13	13.3%	172	8%	3.5 min
SG	121	21%	42	40%	52	25.7%	25	66.6%	110	26.6%	11.8 min
SA	128	28%	15	50%	96	37.1%	4	73.3%	98	34.6%	21.5 min

TABLE IV: Table showing the actual and reconstructed load impedances for the network of Fig. 3 (c) with the computational latency.

To sum up, PSO algorithm overshoots the other considered optimization algorithms when implemented in the GOR method. It has surpassed them in terms of length and impedance errors as well as the computational complexity. GA comes in second place with good performance even with complex branched networks. However, SA and SG can only be applied for simple networks composed of no more than 4 branches but can mess-up once several junctions are addressed.

IV. CONCLUSION

In this paper we recalled the GOR method, a technique capable of blindly reconstructing branched TL networks. It is an incorporation of TDR techniques, graph theory and optimization based algorithms. Particularly, the method's ability to retrieve the tested NUT's topology with precise estimates of branch lengths and load impedances using a single testing port is an important feature for fault diagnosis of complex wiring networks.

Several optimization algorithms, namely GA, PSO, SG, and SA have been adopted to solve the inverse problem of the measured TDR response in the GOR method. The objective was to assess the performance of each in terms of computational cost and precision. An experimental setup based on real aeronautical CAN bus networks with an increasing complexity were deployed for the purpose. Results obtained have shown the ability of all algorithms to reconstruct the right topology. However, PSO outperformed other algorithms with a significant few mm error for branch lengths and several ohms for load impedances when testing a complex network composed of 7 branches interconnected by 2 junctions. More importantly was the few minutes it took to execute the whole process. In fact, this makes it well-suited for future implementation of real-time monitoring.

Future work will need to deal with the applicability of the presented techniques for a complete network scanning under

unstable network circumstances manifested by the presence of vibrations, noise, etc.. Besides, executing the technique while the NUT is normally operating shall be very interesting.

REFERENCES

- [1] F. Auzanneau, "Wire troubleshooting and diagnosis: Review and perspectives," *Progress In Electromagnetics Research*, vol. 49, pp. 253–279, 2013.
- [2] C. Furse, Y. C. Chung, C. Lo, and P. Pendayala, "A critical comparison of reflectometry methods for location of wiring faults," *Smart Structures and Systems*, vol. 2, no. 1, pp. 25–46, 2006.
- [3] P. Smith, C. Furse, and J. Gunther, "Analysis of spread spectrum time domain reflectometry for wire fault location," *IEEE sensors journal*, vol. 5, no. 6, pp. 1469–1478, 2005.
- [4] C. Furse, Y. C. Chung, R. Dangol, M. Nielsen, G. Mabey, and R. Woodward, "Frequency-domain reflectometry for on-board testing of aging aircraft wiring," *IEEE Transactions on Electromagnetic Compatibility*, vol. 45, no. 2, pp. 306–315, 2003.
- [5] C. Buccella, M. Feliziani, and G. Manzi, "Detection and localization of defects in shielded cables by time-domain measurements with uwb pulse injection and clean algorithm postprocessing," *IEEE Transactions on Electromagnetic Compatibility*, vol. 46, no. 4, pp. 597–605, 2004.
- [6] C. Furse, P. Smith, C. Lo, Y. C. Chung, P. Pendayala, and K. Nagoti, "Spread spectrum sensors for critical fault location on live wire networks," *Structural Control and Health Monitoring: The Official Journal of the International Association for Structural Control and Monitoring and of the European Association for the Control of Structures*, vol. 12, no. 3-4, pp. 257–267, 2005.
- [7] L. A. Griffiths, R. Parakh, C. Furse, and B. Baker, "The invisible fray: A critical analysis of the use of reflectometry for fray location," *IEEE Sensors Journal*, vol. 6, no. 3, pp. 697–706, 2006.
- [8] L. Abboud, A. Cozza, and L. Pichon, "A matched-pulse approach for soft-fault detection in complex wire networks," *IEEE Transactions on Instrumentation and Measurement*, vol. 61, no. 6, pp. 1719–1732, 2012.
- [9] M. Kafal, R. Razzaghi, A. Cozza, F. Auzanneau, and W. B. Hassen, "A review on the application of the time reversal theory to wire network and power system diagnosis," in *2019 IEEE International Instrumentation and Measurement Technology Conference (I2MTC)*. IEEE, 2019, pp. 1–6.
- [10] S. Blum, M. Ulrich, and B. Yang, "A continuous cost function for the reconstruction of wired networks from reflection measurements," in *2017 25th European Signal Processing Conference (EUSIPCO)*. IEEE, 2017, pp. 2551–2555.
- [11] Q. Shi and O. Kanoun, "Identification of wire network topology using impedance spectroscopy," in *Proc. 19th Symp. IMEKO*, 2013, pp. 372–377.
- [12] M. K. Smail, L. Pichon, M. Olivas, F. Auzanneau, and M. Lambert, "Reconstruction of faulty wiring networks using reflectometry response and genetic algorithms," *International Journal of Applied Electromagnetics and Mechanics*, vol. 35, no. 1, pp. 39–55, 2011.
- [13] H. Boudjefdjouf, R. Mehasni, A. Orlandi, H. Boucekara, F. De Paulis, and M. Smail, "Diagnosis of multiple wiring faults using time-domain reflectometry and teaching-learning-based optimization," *Electromagnetics*, vol. 35, no. 1, pp. 10–24, 2015.
- [14] H. Boucekara, M. Smail, and G. Dahman, "Diagnosis of multi-fault wiring network using time-domain reflectometry and electromagnetism-like mechanism," *Electromagnetics*, vol. 33, no. 2, pp. 131–143, 2013.
- [15] M.-K. Smail, T. Hacib, L. Pichon, and F. Loete, "Detection and location of defects in wiring networks using time-domain reflectometry and neural networks," *IEEE Transactions on Magnetics*, vol. 47, no. 5, pp. 1502–1505, 2011.
- [16] M. Kafal, J. Benoit, and E. Cabanillas, "Blind diagnosis of a black-boxed fully-loaded wiring network for configuration structuring and fault monitoring," in *2018 IEEE International Instrumentation and Measurement Technology Conference (I2MTC)*. IEEE, 2018, pp. 1–6.
- [17] M. Kafal, F. Mustapha, W. B. Hassen, and J. Benoit, "A non destructive reflectometry based method for the location and characterization of incipient faults in complex unknown wire networks," in *2018 IEEE AUTOTESTCON*. IEEE, 2018, pp. 1–8.
- [18] J. Benoit and M. Kafal, "Procède, mis en oeuvre par ordinateur, de reconstruction de la topologie d'un reseau de cables, utilisant un algorithme genetique," 2018, wO2019030246A1. [Online]. Available: <https://patents.google.com/patent>
- [19] C. R. Paul, *Analysis of multiconductor transmission lines*. John Wiley & Sons, 2007.
- [20] K. Lu, "An efficient method for analysis of arbitrary nonuniform transmission lines," *IEEE Transactions on Microwave Theory and Techniques*, vol. 45, no. 1, pp. 9–14, 1997.
- [21] D. B. West *et al.*, *Introduction to graph theory*. Prentice hall Upper Saddle River, NJ, 1996, vol. 2.
- [22] M. E. Newman, "The structure and function of complex networks," *SIAM review*, vol. 45, no. 2, pp. 167–256, 2003.
- [23] A. Tarantola, *Inverse problem theory and methods for model parameter estimation*. siam, 2005, vol. 89.
- [24] E. Polak, *Optimization: algorithms and consistent approximations*. Springer Science & Business Media, 2012, vol. 124.
- [25] T. Weise, "Global optimization algorithms-theory and application," *Self-Published Thomas Weise*, 2009.
- [26] M. Kafal, J. Benoit, and C. Layer, "A joint reflectometry-optimization algorithm for mapping the topology of an unknown wire network," in *2017 IEEE SENSORS*. IEEE, 2017, pp. 1–3.
- [27] W. B. Hassen, M. Kafal, E. Cabanillas, and J. Benoit, "Power cable network topology reconstruction using multi-carrier reflectometry for fault detection and location in live smart grids," in *2018 Condition Monitoring and Diagnosis (CMD)*. IEEE, 2018, pp. 1–5.
- [28] L. Davis, "Handbook of genetic algorithms," 1991.
- [29] J. Kennedy and R. Eberhart, "Particle swarm optimization (psa)," in *Proc. IEEE International Conference on Neural Networks, Perth, Australia*, 1995, pp. 1942–1948.
- [30] K. Lange, D. R. Hunter, and I. Yang, "Optimization transfer using surrogate objective functions," *Journal of computational and graphical statistics*, vol. 9, no. 1, pp. 1–20, 2000.
- [31] P. J. Van Laarhoven and E. H. Aarts, "Simulated annealing," in *Simulated annealing: Theory and applications*. Springer, 1987, pp. 7–15.